BIODIVERSITAS
Volume 24, Number 5, May 2023
Pages: 2666-2673

ISSN: 1412-033X
E-ISSN: 2085-4722
DOI: 10.13057/biodiv/d240519

The antioxidant potential of copper oxide nanoparticles synthesized from a new bacterial strain

HASAN GHALI ABDULHASAN ALSHAMI[1,♥], WIJDAN H. AL-TAMIMI[1], RASHID RAHIM HATEET[2]

[1]Department of Biology, College of Science, University of Basrah. Basrah, Iraq. Tel./fax.: +96-47722993655, ♥email: pgs2100@uobasrah.edu.iq
[2]Department of Biology, College of Science, University of Misan. Maysan, Iraq

Manuscript received: 7 February 2023. Revision accepted: 15 May 2023.

Abstract. *Alshami HGA, Al-Tamimi WH, Hateet RR. 2023. The antioxidant potential of copper oxide nanoparticles synthesized from a new bacterial strain. Biodiversitas 24: 2666-2673.* Copper oxide nanoparticles (CuONPs) have recently gained much attention due to their potential in various fields. The present study aimed to screen nine bacterial strains (*Klebsiella quasipneumoniae* KP18-31, *K. pneumoniae* IOB-L, *K. quasipneumoniae* subsp. *similipneumoniae* 2437, *Bacillus cereus* DBA1, *B. thuringiensis* MSP51, *Neobacillus drentensis* ROA042, *Enterococcus faecalis* 2674, *Exiguobacterium mexicanum* AB201, and *Acinetobacter lwoffii* K34) isolated from produced water of oil field reservoirs for their ability to biosynthesize CuONPs, as well as characterize and evaluate the antioxidant potential of the manufactured CuONPs. Biosynthesized CuONPs were characterized using XRD, TEM, AFM, and zeta potential analysis. In addition, the DPPH method was used to analyze the antioxidant activity of CuONPs. The results revealed that five of the nine isolates could synthesize CuONPs. *B. thuringiensis* MSP5 was the best and most productive among them, and it was used for the first time in this present study as an oil field bacteria for the biosynthesis of CuONPs. The results showed that CuONPs have a spherical shape with an average size of 20, 33, and 75 nm based on XRD, TEM, and AFM analysis, respectively. The zeta potential value of the synthesized CuONPs was -12.4 mV. The antioxidant results demonstrated that CuONPs have a remarkable scavenging activity with an IC_{50} value of 141.68 μg/mL. This study concluded that CuONPs were excellent free radical scavengers.

Keywords: Antioxidant, bacteria, biosynthesis, characterization, copper oxide nanoparticles

INTRODUCTION

The prevalence of bacteria in deep habitats is well known and includes a diverse range of mesophilic/ thermophilic bacteria, and archaea, many of which can metabolize organic and inorganic substances (Silva et al. 2013). Many studies currently concentrate on harsh environments, as bacteria that live in these places are believed to be adapted to these environments and contain enzymatic systems that might be significant in scientific and commercial applications (Silva et al. 2013; Aboud et al. 2021).

Nanotechnology creates various nanoscale materials of 1-100 nm size in at least one dimension, known as nanomaterials or Nanoparticles (NPs) (Nadeem et al. 2020). Nanotechnology is a modern technique that includes the production, characterization, and application of NPs (Khan et al. 2017). Due to the fabrication and various applications of NPs in multiple fields, nanotechnology has evolved significantly in recent decades; for example, used in biology, agriculture, engineering, electronics, cosmetics, medicine, and biomedical devices (Slavin et al. 2017; Khan et al. 2019).

NPs can be synthesized using bacteria (Mahmoud et al. 2016), yeast (Liu et al. 2021), actinobacteria (Kuyukina et al. 2022), fungi (Al-Timimi et al. 2016), microalgae (Hamida et al. 2022), and plant extracts (De et al. 2020; Rahmah et al. 2023). Recent research has focused on bacterial NP synthesis because of several properties, including the simplicity of cultivating bacteria, synthesis of extracellular NPs, and easy experimental settings such as pH, temperature, and short generation period (Jang et al. 2015). In addition, bacterial cells play a major role in transforming heavy metals into NPs. The synthesis of NPs is associated with multiple functional mechanisms within bacterial cells. Another advantage is their capacity to synthesize large quantities of long-lasting NPs (Fariq et al. 2017). Therefore, using extracellular and intracellular methods, many bacteria have been utilized to synthesize NPs such as silver, gold, copper, copper oxide, and other NPs. Extracellular synthesis occurs when enzymes or biomolecules on the cell's outer surface reduce metal ions, whereas intracellular synthesis occurs within microbial cells (Fouda et al. 2020). For example, Abd-Elhalim (2019) reported that *Pseudomonas silesiensis* could synthesize copper NPs (CuNPs) in two ways, extracellular and intracellular. El-Shanshoury et al. (2020) used four bacterial strains: *Escherichia coli* ATCC 8739, *Bacillus subtilus* ATCC 6633, *Lactobacillus acidophilus* DSMZ 20079T and *Streptococcus thermophiles* ESH1 for the extracellular synthesis of gold NPs (AuNPs). However, extracellular synthesis of NPs is preferred over intracellular synthesis because the manufactured NPs can be easily purified and retrieved (Alfryyan et al. 2022; Wang et al. 2022).

Copper oxide (CuO) is a smart transition metal oxide with a band gap of 2.0 eV and distinct features at the nanoscale, including improved electrochemical activity, a large surface area, suitable redox potential, and amazing stability in solution (Giri and Sarkar 2016). CuONPs are the simplest member of the Cu family (Reddy 2017), easier to make, and have lower costs than gold and other NPs (Rad et al. 2018). The

emergence of nanotechnology in biomedical research causes a remarkable increase in scientific activities that involve CuONPs. CuO has demonstrated pharmacological properties, particularly in anticancer and antibacterial therapy (Kouhkan et al. 2019). Moreover, Talebian et al. (2023) explored CuONPs produced by *Stenotrophomonas* sp. BS95 possesses antibacterial, antioxidant, and anticancer potentials.

Free radicals are significant contributors to the development of degenerative diseases in the body, such as heart and blood vessel disease, mutations, senescence, and cancer (Mujaddidi et al. 2021). Free radicals are defined as molecules or molecular fragments with one or more unpaired electrons in atomic or molecular orbitals that are unstable and highly reactive (Qazi et al. 2018; Martemucci et al. 2022). Antioxidants are substances that interact with free radicals and prevent them from harming cellular components. The source of antioxidants may be natural or synthetic, while NPs are considered synthetic antioxidants (Flieger et al. 2021).

According to our review of previous studies (El-Ghwas 2022; Fouda et al. 2022; Talebian et al. 2023), different environmental sources were selected to isolate bacteria and produce NPs from them. However, no local study has previously employed bacteria from Al-Halfaya oil field reservoirs in Missan governorate, south of Iraq (31°42′ N 47°19′ E), for this purpose. In addition, this is the first report on the biosynthesis of CuONPs using *B. thuringiensis* MSP5. Therefore, the present study aimed to screen bacteria from oil field reservoirs for their ability to biosynthesize CuONPs, characterize the produced CuONPs and assess the antioxidant potential of the synthesized CuONPs.

MATERIALS AND METHODS

Bacterial screening

The previous study identified nine different bacterial strains using universal primers (16S rRNA gene) after being isolated from produced water samples of oil field reservoirs (Alshami et al. 2022). These strains include *Klebsiella quasipneumoniae* KP18-31 (P3), *K. pneumoniae* IOB-L (P4), *K. quasipneumoniae* subsp. *similipneumoniae* 2437 (T11), *Bacillus cereus* DBA1 (P10), *B. thuringiensis* MSP51 (P9), *Neobacillus drentensis* ROA042 (T1), *Enterococcus faecalis* 2674 (P11), *Exiguobacterium mexicanum* AB201 (T8), and *Acinetobacter lwoffii* K34 (T10). In the present study, all bacterial strains were screened for their ability to synthesize CuONPs by observing visible color changes, analyzing samples by UV-visible spectroscopy, and weighing the product (nanopowder) obtained from each bacteria.

The bacteria were cultured in flasks with 50 mL of sterile Nutrient Broth (NB) and incubated in an orbital shaker (150 rpm) at 37°C for 24 h. The cultures were then centrifuged at 6,000 rpm for 10 min using a tabletop centrifuge (Gemmy, Taiwan), and the supernatants were harvested. The supernatant of each isolate was mixed with 50 mL of a 1 mM copper sulfate pentahydrate ($CuSO_4.5H_2O$) solution in 250 mL flasks and then incubated at 37°C for three days at 150 rpm. A mixture of the medium and 1mM $CuSO_4.5H_2O$ solution was used as the control. Visual inspection was done to observe if the color of the supernatant changed during the biosynthesis of CuONPs (Nabila and Kannabiran 2018).

Furthermore, 2 mL of each supernatant that changed color was poured into quartz cuvettes, and the absorbance (Abs) (in the range of 200-800 nm) was measured using the Dual Beam UV-1800 Spectrophotometer instrument (Shimadzu, Japan).

Samples were centrifuged for 10 minutes at 10,000 rpm after the measurement of Abs, and the supernatants were discarded. The precipitates (CuONPs) were washed three times using deionized water, air-dried, collected in powder form, and then weighed (Valentina 2022).

Characterization of the synthesized CuONPs

X-Ray Diffraction (XRD) analysis

Synthesized CuONPs were measured using an X'pert Pro X-ray diffractometer (PANalytical, Netherlands). The diffraction pattern of the powdered form of synthesized NPs was recorded from 10º to 80º (2 thetas), with a step size of 0.050°, by Cu K-Alpha radiation (λ = 1.54060 Å) and operating at 40 kV and 30 mA. Scherer's equation was applied to find the average crystalline size of the NPs (Qais et al. 2019).

Transmission Electron Microscopy (TEM) analysis

The shape, size, and distribution of produced CuONPs were characterized using TEM (Hitachi, Japan). Therefore, to prepare the TEM grid, the suspension of NPs was transferred onto a copper grid covered with carbon. Before imaging, the grid was dried by air, and then individual images were taken at 200 kV using TEM (Qais et al. 2019).

Atomic Force Microscopy (AFM) analysis

The AFM instrument (Nanosurf easyScan 2 AFM, Switzerland) was used to determine the morphology and size of fabricated CuONPs. A thin film of bio-fabricated AgNPs was coated on a clean glass coverslip before AFM scanning and allowed to dry at room temperature (Kotakadi et al. 2016).

Zeta potential measurement

The zeta potential approach was used to evaluate the stability of manufactured CuONPs using a zeta potential analyzer device (HORIBA Scientific SZ-100, Japan). The sample was centrifuged, and the potential was measured between -200 and +200 mV at 25.2°C (Pallavi et al. 2022).

Antioxidant potential of the synthesized CuONPs

The antioxidant potential of CuONPs was assessed in terms of radical scavenging activity using the 1,1-diphenyl-2- picrylhydrazyl (DPPH) test, as described previously (Mujaddidi et al. 2021). First, different concentrations (5, 10, 25, 50, 100, 200, and 400 µg/mL) of CuONPs were prepared in Dimethyl Sulfoxide (DMSO) solution. Next, 1 mL of a 0.004% methanolic DPPH free radical solution was added to 1 mL of each concentrate in glass test tubes. The test tubes were then incubated in the dark at room temperature for 30 minutes, and Abs at 517 nm were measured using a spectrophotometer (EMC LAB, Germany). Ascorbic acid was the positive control, while the DPPH/DMSO solution mixture was the negative control. The antioxidant activity of CuONPs was estimated by the following formula:

$$\text{Antioxidant activity \%} = [(\text{Abs of control} - \text{Abs of sample}) / \text{Abs of control}] \times 100 \ldots\ldots (1)$$

Statistical analysis

The DPPH assay was conducted in triplicate for CuONPs and the control. The data were analyzed using Statistical Package for the Social Sciences (SPSS) software version 26 to determine mean values, standard deviation (means ± SD), and significance between means. Data were analyzed using Analysis of Variance (ANOVA), and $p \leq 0.05$ was deemed statistically significant. The graphs were plotted using the Origin Pro 2018 software.

RESULTS AND DISCUSSION

Bacterial screening

The species' potential to produce CuONPs was first tested by observing the color change during incubation. The results revealed that five out of nine species changed the color of the supernatant from blue to green or dark green, including *N. drentensis* ROA042 (T1), *K. quasipneumoniae* subsp. *similipneumoniae* 2437 (T11), *B. cereus* DBAl (P10), *B. thuringiensis* MSP51 (P9), and *K. quasipneumoniae* KP18-31 (P3). Furthermore, *K. pneumoniae* IOB-L (P4), *E. faecalis* 2674 (P11), *E. mexicanum* AB201 (T8), and *A. lwoffii* K34 (T10) (Table 1), when incubated at the same conditions, exhibited no color change (Figure 1).

The color change noted in the reaction medium demonstrates the production of CuONPs and is also caused by the excitation of Surface Plasmon Resonance (SPR) of CuONPs (Nabila and Kannabiran 2018). These outcomes agree with the findings of Bukhari et al. (2021), who noted that the color of the reaction mixture changed from blue to dark green when *Streptomyces* MHM38 supernatant was added to the $CuSO_4$ solution. Similarly, Fouda et al. (2022) reported that the color of the supernatant of *Brevibacillus brevis* was changed from blue to green after mixing with the precursor, indicating the synthesis of CuONPs. Moreover, Taran et al. (2017) found that the supernatant of *Bacillus* sp. FU4 altered from blue to light green after mixing with $CuSO_4.5H_2O$ solution. Mahmoud et al. (2016) synthesized silver nanoparticles (AgNPs) from bacteria using the same screening method, and the *B. subtilis* strain showed the best results. Screening for the biosynthesis of zinc oxide nanoparticles (ZnONPs) by observing visible color changes in the supernatant of different bacteria was also carried out (El-Ghwas 2022). He noted that only *Bacillus foraminis* could change the color of the supernatant and synthesize ZnONPs.

The UV-visible spectrum of the reaction mixtures was used to confirm the biosynthesis of CuONPs. The five strains that caused the reaction mixes to turn green or dark green underwent testing. In the UV-visible spectrum, peaks at 313 nm, 313 nm, 313 nm, 314 nm, and 318 nm were observed for NPs synthesized using the culture supernatant of *B. thuringiensis* MSP51, *B. cereus* DBA1, *K. quasipneumoniae* subsp. *similipneumoniae* 2437, *N. drentensis* ROA042, and *K. quasipneumoniae* KP18-31, respectively (Figure 2). That was also related to the SPR of CuO, which its peak position is influenced by the size and shape of the NPs synthesized (Rasool and Hemalatha 2017).

Table 1. Screening for the biosynthesis of CuONPs by bacterial species

Isolate code	Name of bacteria	Accession no.	Color change	Absorbance (a.u.)	Wavelength (nm)	Weight of CuONPs powder (mg)
P3	*K. quasipneumoniae* KP18-31	CP045641	Green	0.23	318	2.8
P4	*K. pneumoniae* IOB-L	MN555336	No			0
P9	*B. thuringiensis* MSP51	MG984081	Dark green	2.36	313	11
P10	*B. cereus* DBA1	MT332156	Dark green	2.03	313	6.8
P11	*E. faecalis* 2674	MT611693	No			
T1	*N. drentensis* ROA042	MT525288	Dark green	1.36	314	5.4
T8	*E. mexicanum* AB201	MT436082	No			0
T10	*A. lwoffii* K34	MK548539	No			0
T11	*K. quasipneumoniae* subsp. *similipneumoniae* 2437	MT604862	Dark green	1.75	313	6

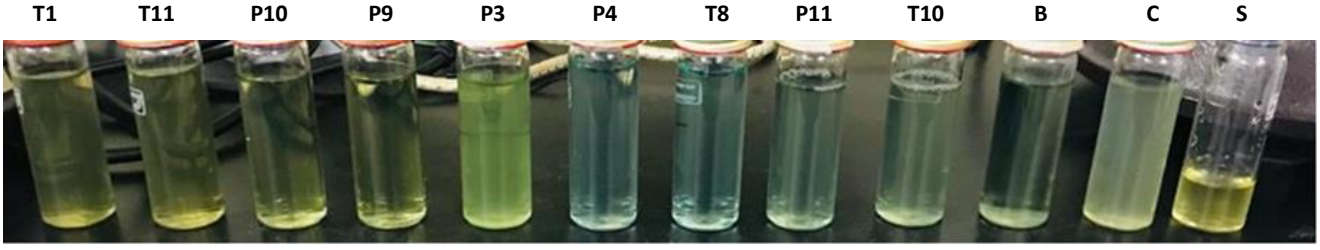

Figure 1. The color change of the culture supernatant of the nine strains treated with (1 mM) $CuSO_4.5H_2O$ solution. T1: *N. drentensis* ROA042, T11: *K. quasipneumoniae* subsp. *similipneumoniae* 2437, P10: *B. cereus* DBA1, P9: *B. thuringiensis* MSP51, P3: *K. quasipneumoniae* KP18-31, P4: *K. pneumoniae* IOB-L, T8: *E. mexicanum* AB201, P11: *E. faecalis* 2674, T10: *A. lwoffii* K34, B: Supernatant treated with $CuSO_4.5H_2O$ solution before incubation, C: Control (medium with only $CuSO_4.5H_2O$ solution), S: Supernatant only

Eltarahony et al. (2018) discovered that the intracellular and extracellular CuONPs manufactured by *Proteus mirabilis* had maximal SPR absorption peaks at 275 and 430 nm, respectively. Spectral analysis in other studies showed that the SPR peaks of CuONPs occurred at 365 nm (Ghorbani et al. 2015), 246 nm (Qamar et al. 2020), 290 nm (Fouda et al. 2022), 400 nm (Hassan et al. 2019), and 337 nm (Sathiyavimal et al. 2018).

The results of the UV-visible spectrum analysis of CuONPs in the present study also exhibited a single peak for each of the five tested strains. The emergence of a single peak in the UV spectra of biosynthesized CuONPs suggests the spherical shape of NPs, as mentioned in the previous studies (Jayakumarai et al. 2015; Nabila and Kannabiran 2018), which is supported by the TEM image.

The screening results revealed that the best results in the development of the dark green color in solution were achieved in *B. thuringiensis* MSP51, with the highest absorbance (2.36) and the peak in the range of CuONPs (313 nm). In addition, it produced excessive amounts of nanopowder (the yield = 11 mg) compared to the other bacteria screened. This strain was previously deposited in GenBank as a new strain (*B. thuringiensis* AMHWRB3) with the accession number MZ672038.1 (Alshami et al. 2022), and it was used for the biosynthesis and characterization of CuONPs in the present study.

Characterization of the synthesized CuONPs

The crystallinity of CuONPs synthesized by *B. thuringiensis* AMHWRB3 was evidenced using XRD analysis. The XRD pattern is displayed in Figure 3. The peaks were observed at 2θ = 32.08°, 38.05°, 56.07°, and 65.52° corresponding to (1 1 0), (1 1 1), (0 2 1), and (0 2 2), respectively. The XRD analysis of the synthesized CuONPs corresponded to the Joint Committee on Powder Diffraction Standards (JCPDS) file NO.01-080-1917, which confirmed the crystalline nature of the CuONPs with a monoclinic phase. Additionally, the XRD pattern exhibited three additional peaks (*) at 2θ = 19.51°, 45.15°, and 59.68° that could be related to crude coating agents as previously reported (Hassan et al. 2019; Halder et al. 2022). Furthermore, XRD results in the present study showed that CuONPs peaks are sharp. The capping agents may have stabilized the NPs, resulting in sharp Bragg peaks. Potent Bragg reflections indicate the presence of strong X-ray scattering centers in the crystalline phase, which could be caused by capping agents (Singh et al. 2018).

Scherrer's equation was used to obtain the average crystalline size of CuONPs manufactured by *B. thuringiensis* AMHWRB3 using the peak position and full width at half maximum (FWHM) values from the XRD data:

$$D=\frac{k\lambda}{\beta \cos \theta} \ldots\ldots\ldots \quad (2)$$

Where; D is the crystallite size of the NPs, k is the Scherrer constant, λ is the wavelength of the X-ray source (1.54056 Å) used in XRD patterns, β is the FWHM of the diffraction peaks in radian, and θ is the Bragg angle in radian. Therefore, using the above equation, the average crystallite size of the CuONPs is calculated to be 20 nm. Santhoshkumar and Shanmugam (2020) reported larger CuONPs (35 ± 6 nm) based on a calculation using Scherrer's equation. In another study, the average particle size of CuONPs produced by *Lactobacillus casei* subsp. *casei* was 200 nm (Kouhkan et al. 2019). A prior investigation used Scherrer's equation to calculate the average size of CuONPs synthesized using *Bacillus* sp. FU4 was found to be 64 nm (Taran et al. 2017). These findings are inconsistent with the results of the present study. According to Talebian et al. (2023), the average crystallite size for crude and calcined CuONPs produced by a cell-free extract of *Stenotrophomonas* sp. BS95 was 18.24 nm and 21.30 nm, respectively. These outcomes are in line with the results of the present study.

TEM analysis has been demonstrated as the most accurate tool for determining the morphology of NPs (Huq and Akter 2021). According to the TEM images, CuONPs synthesized by *B. thuringiensis* AMHWRB3 were spherical and polydisperse (Figure 4). Moreover, a histogram of CuONPs size distribution revealed that their sizes ranged from 9 to 80 nm, with an average diameter of 33 nm.

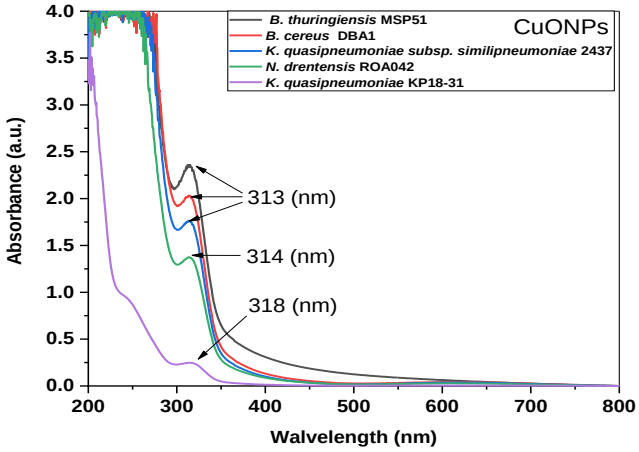

Figure 2. UV Visible-Spectra of CuONPs synthesized by the supernatant of five bacterial strains subjected to the same condition

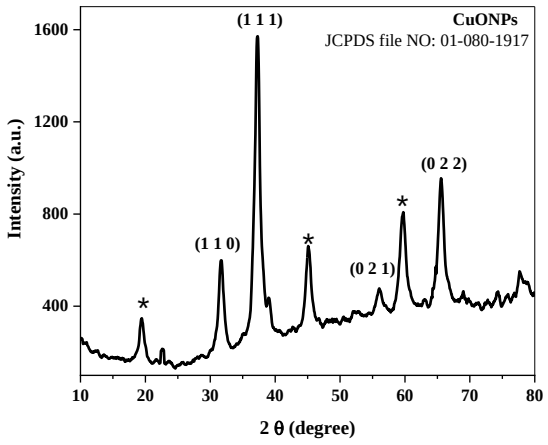

Figure 3. XRD pattern of CuONPs synthesized by *B. thuringiensis* AMHWRB3

In prior work, TEM images of CuONPs manufactured by *Lactobacillus casei* Subsp. *Casei* showed that the particles were spherical, with sizes ranging from 40-110 nm (Kouhkan et al. 2019). Additionally, according to TEM images, Fouda et al. (2022) demonstrated that the CuONPs produced by *Brevibacillus brevis* were spherical, with diameters varying from 2-28 nm and an average size of 10 ± 4 nm. Similar morphology with an average particle size of 100 nm was obtained from CuONPs synthesized using *Bacillus altitudinis* based on a TEM image (Halder et al. 2022). Generally, Physicochemical variables often impact the size and shape of produced NPs. Therefore, to synthesize NPs, several factors must be considered, including pH, time, temperature, and precursor concentration (Marooufpour et al. 2019).

AFM analysis was used to obtain information about the surface topography of CuONPs produced by *B. thuringiensis* AMHWRB3. The two-dimensional (2D) and three-dimensional (3D) AFM images of CuONPs showed that they were spherical, unevenly distributed, and had a mean diameter of about 75 nm (Figure 5). Furthermore, based on AFM imaging, a spherical shape was also produced from *B. altitudinis* CuONPs in a previous study (Halder et al. 2022).

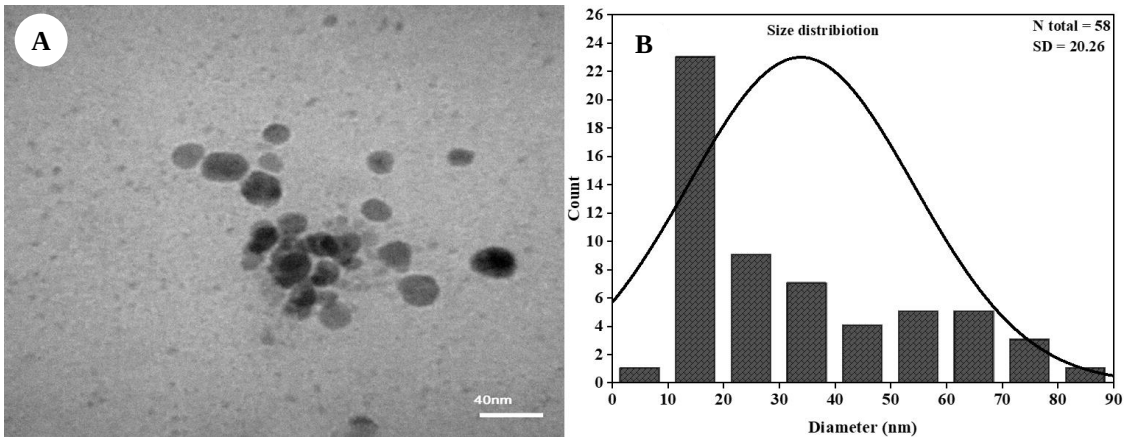

Figure 4. A. The TEM image of CuONPs synthesized using *B. thuringiensis* AMHWRB3; B. particle size distribution histogram

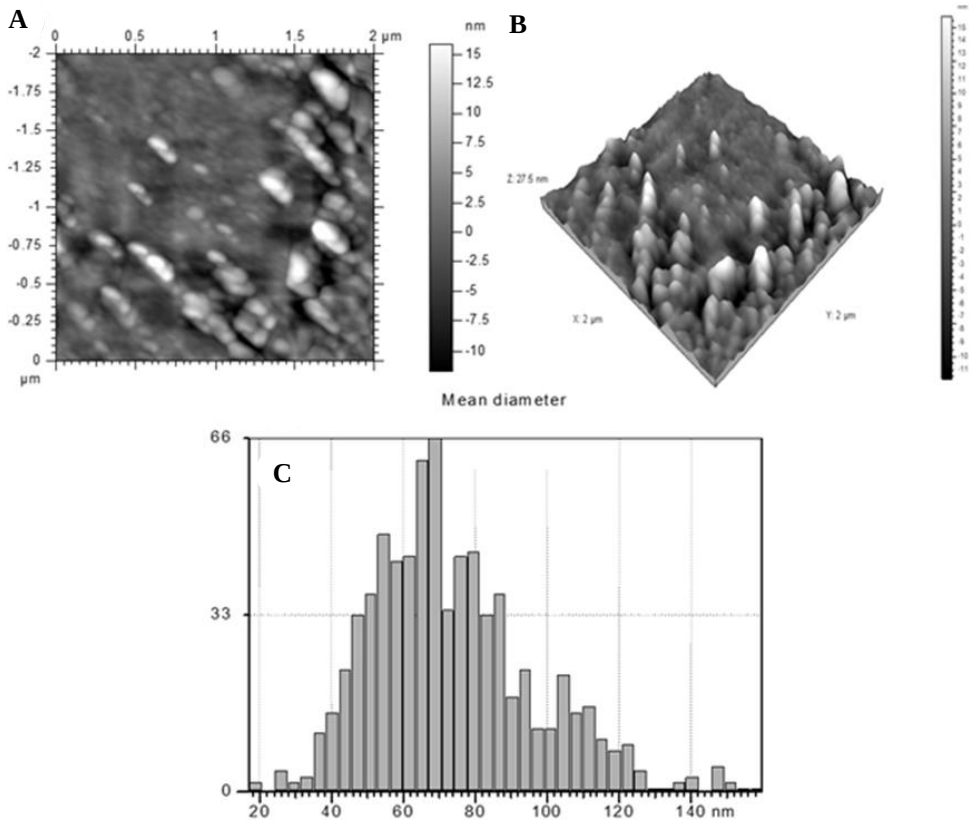

Figure 5. A and B. 2D and 3D images of AFM, respectively; C. The mean diameter of CuONPs synthesized by *B. thuringiensis* AMHWRB3

A Zeta potential analysis was conducted to identify the charge on the surface of synthesized CuONPs, which can be used to evaluate the stability of the produced NPs. The value of the zeta potential shows the possible stability of the NPs. In the present study, the zeta potential of CuONPs was -12.4 mV, indicating the acceptable stability of the synthesized NPs (Figure 6). The charge on their surfaces determines the attraction and repulsive forces between the NPs. Therefore, the long-term stability of NPs depends on their surfaces having a more negative or positive charge since this prevents particle aggregation in the medium (Pallavi et al. 2022).

Compared to the current study, the surface charge of CuO particles produced by *Actinomycetes* was - 31.1 mV (Nabila and Kannabiran 2018), which was more stable. By contrast, *B. altitudinis* produced CuO particles with a zeta potential of -2.26 mV (Halder et al. 2022), less stable than CuONPs synthesized in the present study. However, the stability of the NPs is often influenced by the pH and capping agents (Patil and Chandrasekaran 2020).

Antioxidant potential of the synthesized CuONPs

The antioxidant activity of various concentrations (5, 10, 25, 50, 100, 200, and 400 µg/mL) of synthesized CuONPs compared with ascorbic acid was determined using a DPPH radical scavenging assay. The outcomes demonstrated that CuONPs could scavenge free radicals by changing purple DPPH into yellow (Figure 7), and the inhibition percentage rose with increasing concentration. In methanol solution, DPPH produces a violet or purple color, which turns yellow in the presence of antioxidant agents (Rahman et al. 2015).

The radical is neutralized when it receives a hydrogen atom or an electron from an antioxidant agent. The color shifts from purple to yellow if it is in the reduced state (DPPH-H). The DPPH radical's unpaired electron exhibits significant absorption at 517 nm and a deep purple color. The color decolorizes to yellow when an odd electron pairs with another electron to make it more stable (Yasin et al. 2022).

In the present study, the percentage of scavenging activity of CuONPs in comparison to the control (ascorbic acid) is shown in Table 2. The results revealed significant differences between ascorbic acid and CuONPs (*p*-value = 0.000). Furthermore, the half-maximal inhibitory concentration (IC_{50}) values for CuONPs and ascorbic acid were 16.51 and 141.68 µg/mL, respectively. That indicates CuONPs are less active than ascorbic acid; since the lower the IC_{50} value, the higher the activity.

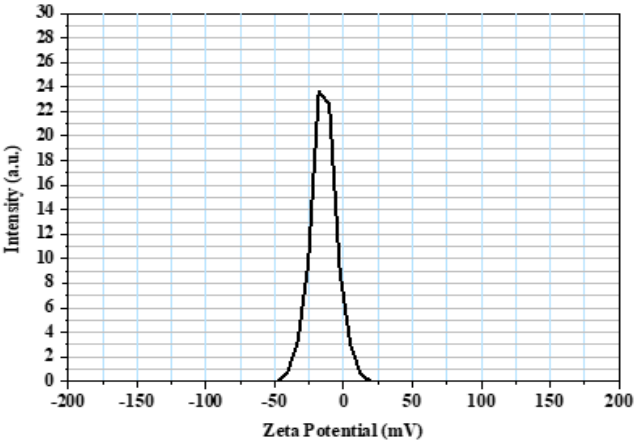

Figure 6. Zeta potential value for CuONPs synthesized using *B. thuringiensis* AMHWRB3

Table 2. The antioxidant activities of CuONPs in comparison to the ascorbic acid

Concentrations (µg/mL)	Antioxidant activity of ascorbic acid (%)	Antioxidant activity of CuONPs (%)	*p*-value
5	34.18±1.18	25.92±1.02	0.000
10	43.01±1.03	29.91±2.89	0.000
25	54.27±1.07	40.88±0.08	0.000
50	61.25±1.15	47.72±3.02	0.000
100	70.94±3.04	53.84±1.75	0.000
200	80.05±1.10	60.68±2.68	0.000
400	92.16±0.96	70.79±3.09	0.000
	IC_{50}= 16.51 µg/mL	IC_{50}= 141.68 µg/mL	

Note: Mean ± SD (n = 3, P ≤ 0.05)

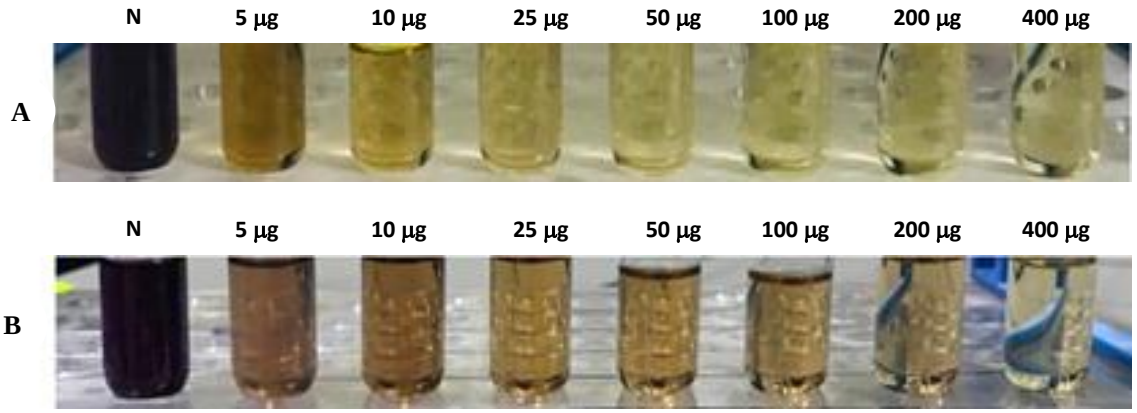

Figure 7. A. DPPH free radical scavenging of ascorbic acid, B. CuONPs at various concentrations (5-400 µg/mL), N: Negative control (DPPH solution/DMSO solution mixture)

In a prior investigation, green synthesized CuONPs exhibited antioxidant activity of 72.5±4.1 and 82.0±1% at 100 and 200 µg/mL doses, respectively (Shalaby et al. 2022). This result does not agree with the present study at the same concentrations. Ssekatawa et al. (2022) revealed that concentrations of 50, 100, and 200 µg/mL from biologically synthesized CuONPs showed antioxidant activity of 17.5, 19.3, and 24.2%, respectively, indicating less radical scavenging activity than the present study. However, the CuONPs produced in the present study have significant antioxidant properties in scavenging free radicals.

In conclusion, the nine isolates of produced water samples were screened for their ability to synthesize CuONPs. Five isolates were able to synthesize CuONPs. However, *B. thuringiensis* AMHWRB3 exhibited the best results. This is the first study on the biosynthesis of CuONPs from oil field reservoirs using this bacterium. Physical characteristics demonstrated that the CuONPs have a spherical shape, are unevenly distributed, and have a size within the NPs range. The present study concluded that CuONPs are powerful free radical scavengers. The biological method for manufacturing NPs is affordable, simple, and environmentally friendly. However, important aspects like organism types, ideal conditions for cell growth and enzymatic activity, and optimal reaction conditions must be considered for the synthesis of highly stable and well-characterized NPs. Moreover, the majority of biomedical research has been conducted *in vitro*. Therefore, it is hoped that microbial NPs will offer enormous promise in medicine with future in-depth studies.

ACKNOWLEDGEMENTS

The authors would like to thank the Colleges of Nursing and Science at the University of Misan, Iraq, for providing the laboratory tools needed to accomplish this work.

REFERENCES

Abd-Elhalim BT, Gamal RF, Abou-Taleb KA, Haroun AA. 2019. Biosynthesis of copper nanoparticles using bacterial supernatant optimized with certain agro-industrial byproducts. Nov Res Microbiol J 3 (6): 558-578. DOI: 10.21608/nrmj.2019.66748.

Aboud EM, Burghal AA, Laftah AH. 2021. Genetic identification of hydrocarbons degrading bacteria isolated from oily sludge and petroleum-contaminated soil in Basrah City, Iraq. Biodiversitas 22 (4): 1934-1939. DOI: 10.13057/biodiv/d220441.

Alfryyan N, Kordy MGM, Abdel-Gabbar M, Soliman HA, Shaban M. 2022. Characterization of the biosynthesized intracellular and extracellular plasmonic silver nanoparticles using *Bacillus cereus* and their catalytic reduction of methylene blue. Sci Rep 12 (1): 12495. DOI: 10.1038/s41598-022-16029-1.

Alshami HGA, Al-tamimi WH, Hateet RR. 2022. Screening for extracellular synthesis of silver nanoparticles by bacteria isolated from Al-Halfaya oil field reservoirs in Missan Province, Iraq. Biodiversitas 23 (7): 3462-3470. DOI: 10.13057/biodiv/d230720.

Al-Timimi IAJ, Sermon PA, Burghal AA, Salih AA, Alrubaya IMN. 2016. Nanoengineering the antibacterial activity of biosynthesized nanoparticles of TiO_2, Ag, and Au and their nanohybrids with Portobello Mushroom Spore (PMS) (TiO x /PMS, Ag/PMS and Au/PMS) and making them optically self-indicating. Proceedings Biosensing and Nanomedicine IX: 99300B. San Diego, California. DOI: 10.1117/12.2237643.

Bukhari SI, Hamed MM, Al-Agamy MH, Gazwi HSS, Radwan HH, Youssif AM. 2021. Biosynthesis of copper oxide nanoparticles using *Streptomyces* MHM38 and its biological applications. J Nanomater 2021: 6693302. DOI: 10.1155/2021/6693302.

De A, Das R, Jain P, Kaur H. 2020. Green chemistry-assisted synthesis of CuO nanoparticles: Reaction optimization, DNA cleavage, and DNA binding studies. Mater Today Proc 49: 3122-3125. DOI: 10.1016/j.matpr.2020.10.955.

El-Ghwas DE. 2022. Short communication: Characterization and biological synthesis of zinc oxide nanoparticles by new strain of *Bacillus foraminis*. Biodiversitas 23 (1): 548-553. DOI: 10.13057/biodiv/d230159.

El-Shanshoury AERR, Ebeid EZE, Elsilk SE, Mohamed SF, Ebeid ME. 2020. Biogenic synthesis of gold nanoparticles by bacteria and utilization of the chemical fabricated for diagnostic performance of viral hepatitis C virus-NS4. Lett Appl NanoBioScience 9 (3): 1395-1408. DOI: 10.33263/LIANBS93.13951408.

Eltarahony M, Zaki S, Abd-El-Haleem D. 2018. Concurrent synthesis of zero- and one-dimensional, spherical, rod-, needle-, and wire-shaped cuo nanoparticles by *proteus mirabilis* 10B. J Nanomater 2018: 1849616. DOI: 10.1155/2018/1849616.

Fariq A, Khan T, Yasmin A. 2017. Microbial synthesis of nanoparticles and their potential applications in biomedicine. J Appl Biomed 15 (4): 241-248. DOI: 10.1016/j.jab.2017.03.004.

Flieger J, Flieger W, Baj J, Maciejewski R. 2021. Antioxidants: Classification, natural sources, activity/capacity measurements, and usefulness for the synthesis of nanoparticles. Materials 14 (15): 4135. DOI: 10.3390/ma14154135.

Fouda A, Hassan SED, Abdo AM, El-Gamal MS. 2020. Antimicrobial, antioxidant and larvicidal activities of spherical silver nanoparticles synthesized by endophytic *Streptomyces* spp. Biol Trace Elem Res 195 (2): 707-724. DOI: 10.1007/s12011-019-01883-4.

Fouda A, Hassan SED, Eid AM, Awad MA, Althumayri K, Badr NF, Hamza MF. 2022. Endophytic bacterial strain, *Brevibacillus brevis*-mediated green synthesis of copper oxide nanoparticles, characterization, antifungal, in vitro cytotoxicity, and larvicidal activity. Green Process Synth 11 (1): 931-950. DOI: 10.1515/gps-2022-0080.

Ghorbani HR, Fazeli I, Fallahi AA. 2015. Biosynthesis of copper oxide nanoparticles using extract of *E. coli*. Orient J Chem 31 (1): 515-517. DOI: 10.13005/ojc/310163.

Giri SD, Sarkar A. 2016. Electrochemical study of bulk and monolayer copper in alkaline solution. J Electrochem Soc 163 (3): H252-H259. DOI: 10.1149/2.0071605jes.

Halder U, Roy RK, Biswas R, Khan D, Mazumder K, Bandopadhyay R. 2022. Synthesis of copper oxide nanoparticles using capsular polymeric substances produced by *Bacillus altitudinis* and investigation of its efficacy to kill pathogenic *Pseudomonas aeruginosa*. Chem Eng J Adv 11: 100294. DOI: 10.1016/j.ceja.2022.100294.

Hamida RS, Ali MA, Almohawes ZN, Alahdal H, Momenah MA, Bin-Meferij MM. 2022. Green synthesis of hexagonal silver nanoparticles using a novel microalgae *Coelastrella aeroterrestrica* strain BA_Chlo4 and resulting anticancer, antibacterial, and antioxidant activities. Pharmaceutics 14 (10): 2002. DOI: 10.3390/pharmaceutics14102002.

Hassan SED, Fouda A, Radwan AA, Salem SS, Barghoth MG, Awad MA, Abdo AM, El-Gamal MS. 2019. Endophytic *actinomycetes Streptomyces* spp. mediated biosynthesis of copper oxide nanoparticles as a promising tool for biotechnological applications. J Biol Inorg Chem 24 (3): 377-393. DOI: 10.1007/s00775-019-01654-5.

Huq MA, Akter S. 2021. Biosynthesis, characterization and antibacterial application of novel silver nanoparticles against drug resistant pathogenic *Klebsiella pneumoniae* and *Salmonella enteritidis*. Molecules 26 (19): 5996. DOI: 10.3390/molecules26195996.

Jang GG, Jacobs CB, Gresback RG, Ivanov IN, Meyer HM, Kidder M, Joshi PC, Jellison GE, Phelps TJ, Graham DE, Moon JW. 2015. Size tunable elemental copper nanoparticles: Extracellular synthesis by thermoanaerobic bacteria and capping molecules. J Mater Chem C 3: 644-650. DOI: 10.1039/c4tc02356k.

Jayakumarai G, Gokulpriya C, Sudhapriya R, Sharmila G, Muthukumaran C. 2015. Phytofabrication and characterization of monodisperse copper oxide nanoparticles using *Albizia lebbeck* leaf extract. Appl Nanosci 5 (8): 1017-1021. DOI: 10.1007/s13204-015-0402-1.

Khan I, Saeed K, Khan I. 2019. Nanoparticles: Properties, applications and toxicities. Arab J Chem 12 (7): 908-931. DOI: 10.1016/j.arabjc.2017.05.011.

Khan ZUH, Khan A, Chen Y, Shah NS, Muhammad N, Khan AU, Tahir K, Khan FU, Murtaza B, Hassan SU, Qaisrani SA, Wan P. 2017. Biomedical applications of green synthesized nobel metal nanoparticles. J Photochem Photobiol B 173: 150-164. DOI: 10.1016/j.jphotobiol.2017.05.034.

Kotakadi VS, Gaddam SA, Venkata SK, Sarma PVGK, Gopal DVRS. 2016. Biofabrication and spectral characterization of silver nanoparticles and their cytotoxic studies on human CD34 +ve stem cells. 3 Biotech 6 (2): 216. DOI: 10.1007/s13205-016-0532-5.

Kouhkan M, Ahangar P, Babaganjeh LA, Allahyari-Devin M. 2019. Biosynthesis of copper oxide nanoparticles using *Lactobacillus casei* subsp. *Casei* and its anticancer and antibacterial activities. Curr Nanosci 16 (1): 101-111. DOI: 10.2174/1573413715666190318155801.

Kuyukina MS, Makarova MV, Ivshina IB, Kazymov KP, Osovetsky BM. 2022. Biosynthesis and characterization of Gold nanoparticles produced using *Rhodococcus actinobacteria* at elevated chloroauric acid concentrations. Intl J Mol Sci 23 (21): 12939. DOI: 10.3390/ijms232112939.

Liu X, Chen JL, Yang WY, Qian YC, Pan JY, Zhu CN, Liu L, Ou WB, Zhao HX, Zhang DP. 2021. Biosynthesis of silver nanoparticles with antimicrobial and anticancer properties using two novel yeasts. Sci Rep 11 (1): 15795. DOI: 10.1038/s41598-021-95262-6.

Mahmoud WM, Abdelmoneim TS, Elazzazy AM. 2016. The impact of silver nanoparticles produced by *Bacillus pumilus* as antimicrobial and nematicide. Front Microbiol 7: 1746. DOI: 10.3389/fmicb.2016.01746.

Marooufpour N, Alizadeh M, Hatami M, Lajayer BA. 2019. Biological synthesis of nanoparticles by different groups of bacteria. In: Prasad, R (ed) Microbial Nanobionics. Nanotechnology in the Life Sciences. Springer, Cham. DOI: 10.1007/978-3-030-16383-9_3.

Martemucci G, Costagliola C, Mariano M, D'andrea L, Napolitano P, D'Alessandro AG. 2022. Free radical properties, source and targets, antioxidant consumption and health. Oxygen 2 (2): 48-78. DOI: 10.3390/oxygen2020006.

Mujaddidi N, Nisa S, Al Ayoubi S, Bibi Y, Khan S, Sabir M, Zia M, Ahmad S, Qayyum A. 2021. Pharmacological properties of biogenically synthesized silver nanoparticles using endophyte *Bacillus cereus* extract of *Berberis lyceum* against oxidative stress and pathogenic multidrug-resistant bacteria. Saudi J Biol Sci 28 (11): 6432-6440. DOI: 10.1016/j.sjbs.2021.07.009.

Nabila MI, Kannabiran K. 2018. Biosynthesis, characterization and antibacterial activity of copper oxide nanoparticles (CuO NPs) from *actinomycetes*. Biocatal Agric Biotechnol 15: 56-62. DOI: 10.1016/j.bcab.2018.05.011.

Nadeem M, Khan R, Afridi K, Nadhman A, Ullah S, Faisal S, Mabood ZU, Hano C, Abbasi BH. 2020. Green synthesis of cerium oxide nanoparticles (CeO_2 nps) and their antimicrobial applications: A review. Intl J Nanomedicine 15: 5951-5961. DOI: 10.2147/IJN.S255784.

Pallavi SS, Rudayni HA, Bepari A, Niazi SK, Nayaka S. 2022. Green synthesis of Silver nanoparticles using *Streptomyces hirsutus* strain SNPGA-8 and their characterization, antimicrobial activity, and anticancer activity against human lung carcinoma cell line A549. Saudi J Biol Sci 29 (1): 228-238. DOI: 10.1016/j.sjbs.2021.08.084.

Patil S, Chandrasekaran R. 2020. Biogenic nanoparticles: A comprehensive perspective in synthesis, characterization, application and its challenges. J Genet Eng Biotechnol 18 (1): 67. DOI: 10.1186/s43141-020-00081-3.

Qais FA, Shafiq A, Khan HM, Husain FM, Khan RA, Alenazi B, Alsalme A, Ahmad I. 2019. Antibacterial effect of silver nanoparticles synthesized using *Murraya koenigii* (L.) against multidrug-resistant pathogens. Bioinorg Chem Appl 2019: 4649506. DOI: 10.1155/2019/4649506.

Qamar H, Rehman S, Chauhan DK, Tiwari AK, Upmanyu V. 2020. Green synthesis, characterization and antimicrobial activity of copper oxide nanomaterial derived from *Momordica charantia*. Intl J Nanomed 15: 2541-2553. DOI: 10.2147/IJN.S240232.

Qazi MA, Molvi KI. 2018. Free radicals and their management. Am J Pharm Health Res 6 (4): 1-10. DOI: 10.46624/ajphr.2018.v6.i4.001.

Rad M, Taran M, Alavi M. 2018. Effect of incubation time, CuSO4 and glucose concentrations on biosynthesis of copper oxide (CuO) nanoparticles with rectangular shape and antibacterial activity: Taguchi method approach. Nano Biomed Eng 10 (1): 25-33. DOI: 10.5101/nbe.v10i1.p25-33.

Rahmah MI, Majdi HS, Al-Azzawi WK, Rasn MJ, Jasim HH, Jabir MS, Alkareem RASA, Rashid TM. 2023. Synthesis of ZnO/Ag-doped C/N heterostructure for photocatalytic application. Intl J Mod Phys B (2023): 2350239. DOI: 10.1142/S0217979223502399.

Rahman MM, Islam MB, Biswas M, Khurshid Alam AHM. 2015. In vitro antioxidant and free radical scavenging activity of different parts of *Tabebuia pallida* growing in Bangladesh. BMC Res Notes 8 (1): 621. DOI: 10.1186/s13104-015-1618-6.

Rasool U, Hemalatha S. 2017. Marine endophytic actinomycetes assisted synthesis of copper nanoparticles (CuNPs): Characterization and antibacterial efficacy against human pathogens. Mater Lett 194: 176-180. DOI: 10.1016/j.matlet.2017.02.055.

Reddy KR. 2017. Green synthesis, morphological and optical studies of CuO nanoparticles. J Mol Struct 1150: 553-557. DOI: 10.1016/j.molstruc.2017.09.005.

Santhoshkumar J, Shanmugam V. 2020. Green synthesis of copper oxide nanoparticles from *Magnolia champaca* floral extract and its antioxidant and toxicity assay using *Danio rerio*. Intl J Recent Technol Eng 8 (5): 5444-5449. DOI: 10.35940/ijrte.e6869.018520.

Sathiyavimal S, Vasantharaj S, Bharathi D, Saravanan M, Manikandan E, Kumar SS, Pugazhendhi A. 2018. Biogenesis of copper oxide nanoparticles (CuONPs) using *Sida acuta* and their incorporation over cotton fabrics to prevent the pathogenicity of Gram negative and Gram positive bacteria. J Photochem Photobiol B 188: 126-134. DOI: 10.1016/j.jphotobiol.2018.09.014.

Shalaby EA, Shanab SMM, El-Raheem WMA, Hanafy EA. 2022. Biological activities and antioxidant potential of different biosynthesized nanoparticles of *Moringa oleifera*. Sci Rep 12 (1): 18400. DOI: 10.1038/s41598-022-23164-2.

Silva TR, Verde LCL, Santos Neto EV, Oliveira VM. 2013. Diversity analyses of microbial communities in petroleum samples from Brazilian oil fields. Intl Biodeterior Biodegrad 81: 57-70. DOI: 10.1016/j.ibiod.2012.05.005.

Singh H, Du J, Singh P, Yi TH. 2018. Extracellular synthesis of silver nanoparticles by *Pseudomonas* sp. THG-LS1.4 and their antimicrobial application. J Pharm Anal 8 (4): 258-264. DOI: 10.1016/j.jpha.2018.04.004.

Slavin YN, Asnis J, Häfeli UO, Bach H. 2017. Metal nanoparticles: Understanding the mechanisms behind antibacterial activity. J Nanobiotechnol 15 (1): 65. DOI: 10.1186/s12951-017-0308-z.

Ssekatawa K, Byarugaba DK, Angwe MK, Wampande EM, Ejobi F, Nxumalo E, Maaza M, Sackey J, Kirabira JB. 2022. Phyto-mediated copper oxide nanoparticles for antibacterial, antioxidant and photocatalytic performances. Front Bioeng Biotechnol 10*:* 820218. DOI: 10.3389/fbioe.2022.820218.

Talebian S, Shahnavaz B, Nejabat M, Abolhassani Y, Rassouli FB. 2023. Bacterial-mediated synthesis and characterization of copper oxide nanoparticles with antibacterial, antioxidant, and anticancer potentials. Front Bioeng Biotechnol 11: 1140010. DOI: 10.3389/fbioe.2023.1140010.

Taran M, Rad M, Alavi M. 2017. Antibacterial activity of copper oxide (CuO) nanoparticles biosynthesized by *bacillus* sp. FU4: Optimization of experiment design. Pharm Sci 23 (3): 198-206. DOI: 10.15171/PS.2017.30.

Valentina Y. 2022. Optimisation of reactant concentration in biosynthesis of silver nanoparticles using pathogenic bacteria isolated from clinical sources and their characterisation: A recent study. Innov Microbiol Biotechnol 3: 45-55. DOI: 10.9734/bpi/imb/v3/1732a.

Wang X, Lee SY, Akter S, Huq MA. 2022. Probiotic-mediated biosynthesis of silver nanoparticles and their antibacterial applications against pathogenic strains of *Escherichia coli* O157:H7. Polymers 14 (9): 1834. DOI: 10.3390/polym14091834.

Yasin A, Fatima U, Shahid S, Mansoor S, Inam H, Javed M, Iqbal S, Alrbyawi H, Somaily HH, Pashameah RA, Alzahrani E, Farouk AE. 2022. Fabrication of copper oxide nanoparticles using *passiflora edulis* extract for the estimation of antioxidant potential and photocatalytic methylene blue dye degradation. Agronomy 12 (10): 2315. DOI: 10.3390/agronomy12102315.